Dynamical geography and transition paths of *Sargassum* in the tropical Atlantic

F. J. Beron-Vera, M. J. Olascoaga, N. F. Putman, et al.

View Online   Export Citation   CrossMark

ARTICLES YOU MAY BE INTERESTED IN

AIP Advances
Fluids and Plasmas Collection
READ NOW
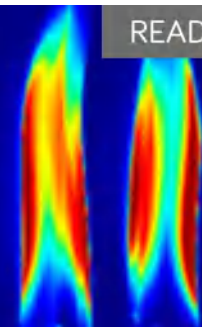
Dynamical geography and transition paths of *Sargassum* in the tropical Atlantic

View Online   Export Citation   CrossMark

F. J. Beron-Vera,[1,a)] (iD) M. J. Olascoaga,[2,b)] (iD) N. F. Putman,[3,c)] (iD) J. Triñanes,[4,5,6] G. J. Goni,[4,f)] and R. Lumpkin[4,g)]

AFFILIATIONS

[1] Department of Atmospheric Sciences, Rosenstiel School of Marine and Atmospheric Science, University of Miami, Miami, Florida 33149, USA
[2] Department of Ocean Sciences, Rosenstiel School of Marine and Atmospheric Science, University of Miami, Miami, Florida 33149, USA
[3] LGL Ecological Research Associates, Inc., Bryan, Texas 77802, USA
[4] Atlantic Oceanographic and Meteorological Laboratory, National Oceanic and Atmospheric Administration, Miami, Florida 33149, USA
[5] Cooperative Institute for Marine & Atmospheric Studies, University of Miami, Miami, Florida 33146, USA
[6] Departamento de Electrónica y Computación, Universidade de Santiago de Compostela, Santiago, Spain

[a)]Author to whom correspondence should be addressed: fberon@miami.edu
[b)]jolascoaga@miami.edu
[c)]nathan.putman@gmail.com
[d)]joaquin.trinanes@noaa.gov
[e)]Also at: Cooperative Institute for Marine & Atmospheric Studies, University of Miami, Miami, Florida 33146, USA and Departamento de Electrónica y Computación, Universidade de Santiago de Compostela, Santiago, Spain.
[f)]gustavo.goni@noaa.gov
[g)]rick.lumpkin@noaa.gov

ABSTRACT

By analyzing a time-homogeneous Markov chain constructed using trajectories of undrogued drifting buoys from the NOAA Global Drifter Program, we find that probability density can distribute in a manner that resembles very closely the recently observed recurrent belt of high *Sargassum* concentration in the tropical Atlantic between 5 and 10°N, coined the *Great Atlantic Sargassum Belt* (*GASB*). A spectral analysis of the associated transition matrix further unveils a forward attracting almost-invariant set in the northwestern Gulf of Mexico with a corresponding basin of attraction weakly connected with the Sargasso Sea but including the nutrient-rich regions around the Amazon and Orinoco rivers mouths and also the upwelling system off the northern coast of West Africa. This represents a data-based inference of potential remote sources of *Sargassum* recurrently invading the Intra-Americas Seas (IAS). By further applying Transition Path Theory (TPT) to the data-derived Markov chain model, two potential pathways for *Sargassum* into the IAS from the upwelling system off the coast of Africa are revealed. One TPT-inferred pathway takes place along the GASB. The second pathway is more southern and slower, first going through the Gulf of Guinea, then across the tropical Atlantic toward the mouth of the Amazon River, and finally along the northeastern South American margin. The existence of such a southern TPT-inferred pathway may have consequences for bloom stimulation by nutrients from river runoff.

I. INTRODUCTION

Since early 2010s, pelagic *Sargassum*, a genus of brown macroalgae that form floating rafts at the ocean surface, has inundated the Intra-American Seas (IAS), particularly the Caribbean Sea, during the spring and summer months (Wang *et al.*, 2019). These rafts of algae serve as important habitats for diverse marine fauna (Bertola *et al.*, 2020) and have been argued to be important carbon sinks (Paraguay-Delgado *et al.*, 2020). Nonetheless, these rafts carry large amounts of toxic substances and heavy metals, and, when they enter coastal zones, they can result in mortality to fishes and sea turtles and effectively smother seagrass and coral communities
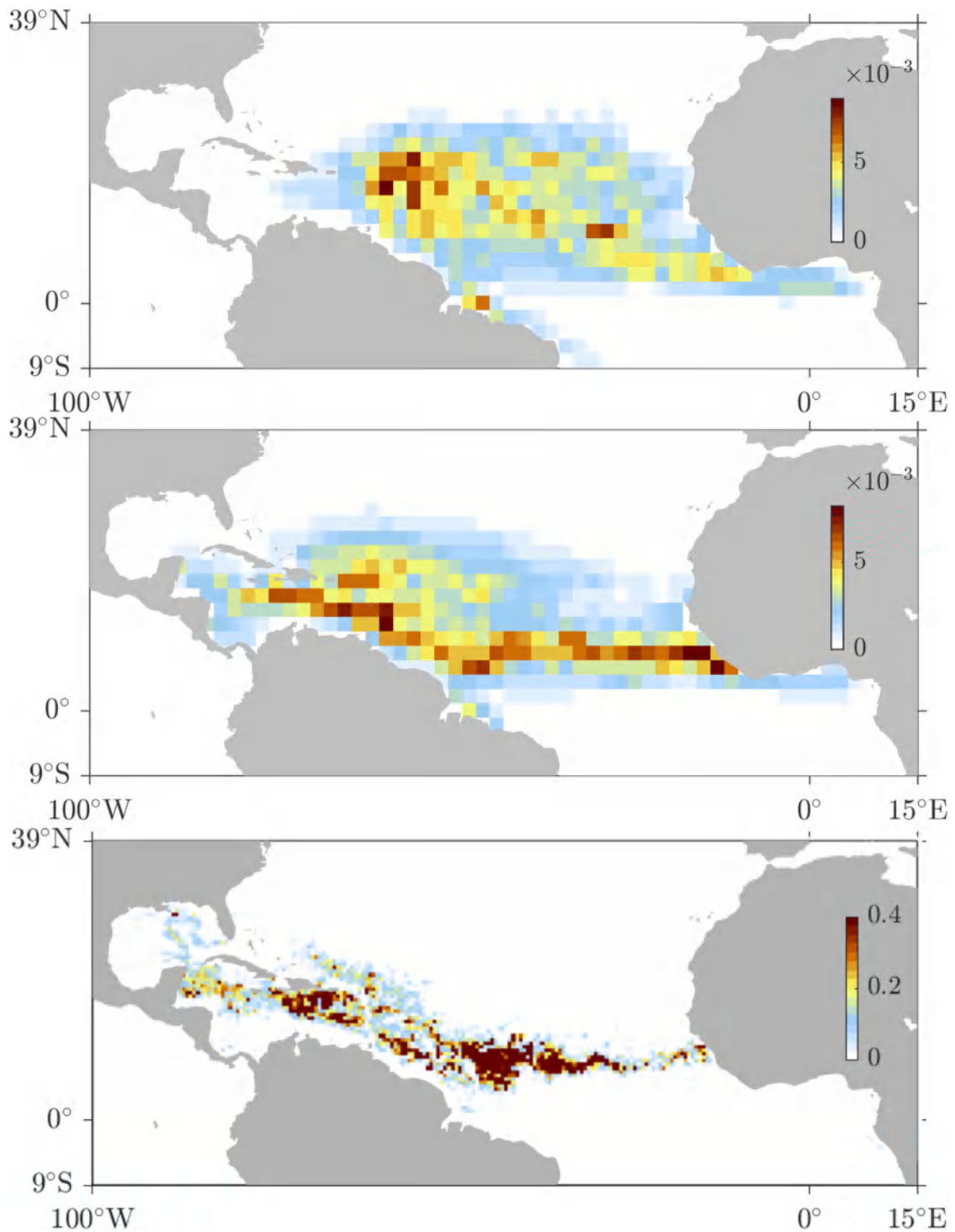
FIG. 1. Starting from a uniform distribution, the discrete probability density of finding tracer after four months of evolution along a Markov chain constructed based on drogued (top panel) and undrogued (middle panel) drifter trajectories from the NOAA Global Drifter Program (GDP). (Bottom panel) The *Great Atlantic Sargassum belt* (*GASB*) as inferred in 2015 from the NASA Moderate Resolution Imaging Spectroradiometer (MODIS) aboard *Terra* and *Aqua* satellites. The quantity plotted is the percentage of *Sargassum* coverage per pixel as determined by the Alternative Floating Algae Index (AFAI), a measure of the magnitude of red edge reflectance of floating *Sargassum*.

(van Tussenbroek *et al.*, 2017). As large *Sargassum* rafts decompose onshore, they give off toxic amounts of hydrogen sulfide that can cause health problems in humans, the volume that washes ashore on beaches also diminishes tourism and, as a result, disrupts the local economy (Smetacek and Zingone, 2013; Resiere *et al.*, 2018).

Comprehensive analyses of satellite imagery across the Atlantic Ocean have revealed a recurrent band of *Sargassum* high density between about 5 and 10°N, referred to as the *Great Atlantic Sargassum Belt* (*GASB*) in Wang *et al.* (2019), often extending off the coast of West Africa to the Gulf of Mexico (Fig. 1, bottom panel). The factors that precipitated blooms of pelagic *Sargassum* in the tropical Atlantic remain an area of active debate, as do the factors that maintain its occurrence across this region (Jouanno *et al.*, 2021b; 2021a; and Lapointe *et al.*, 2021). Several published studies have attempted to account for the spatiotemporal variability in its distribution by simulating the movement of *Sargassum* rafts as passive tracers advected by surface velocity fields produced by ocean circulation models. Conclusions about the connectivity between *Sargassum* blooms in the tropical Atlantic and the Sargasso Sea fundamentally differ depending on whether simulations assume winds contribute to *Sargassum* movement (Franks *et al.*, 2016; Wang *et al.*, 2019; and Johns *et al.*, 2020). Available empirical data suggest that accounting for windage effects improves predictions of *Sargassum* raft trajectories (Putman *et al.*, 2020) and distribution (Berline *et al.*, 2020).

The importance of windage in modeling *Sargassum* movement is demonstrated in the top and middle panels of Fig. 1, which show discrete probability densities of finding *Sargassum* in the tropical Atlantic after three months of evolution from an initially uniform distribution inside $\mathscr{I} = [5°S, 18°N] \times [58°W, 15°W]$ as in Wang *et al.* (2019). Unlike Wang *et al.* (2019) and earlier work, which resorted to tracer advection by simulated velocity, the evolution is here provided by a transfer operator (Lasota and Mackey, 1994) obtained by discretizing (Ulam, 1960) the motion as described by the trajectories $x(t)$ of surface drifting buoys from the National Oceanic and Atmospheric Administration (NOAA) Global Drifter Program (GDP) (Lumpkin and Pazos, 2007) assuming that the underlying dynamics represent a passive advection–diffusion process [e.g. Miron *et al.* (2019a)].

The discrete transfer operator is given by a *transition matrix* $\mathbb{P} = (P_{ij}) \in \mathbb{R}^{N \times N}$ of conditional probabilities of $x(t)$ to moving between nonintersecting boxes $\{b_1, \ldots, b_N\}$ covering the surface of the Atlantic between 9°S and 39°N, denoted $\mathscr{D}$, viz.,

$$P_{ij} = \mathrm{prob}(X_{n+1} \in b_j \mid X_n \in b_i) \approx \frac{C_{ij}}{\sum_{k=1}^{N} C_{ik}}, \tag{1a}$$

where

$$C_{ij} := \#\{x(t) \in b_i, \, x(t+T) \in b_j\}, \tag{1b}$$

independent of the start time t. Here, X_n denotes random position at discrete time nT, where T is the *transition time step*. The boxes represent the states of a *Markov chain*, namely, a stochastic model describing the stochastic state transitions in which the transition probability of each state depends only on the state attained in the previous event (Norris, 1998). By ignoring the start time t of a trajectory in (1), the chain is rendered time-homogeneous.

The evolution of $\mathrm{prob}(X_n \in b_i)$ is obtained under left multiplication by $\mathbb{P}$, i.e.,

$$\mathrm{prob}(X_{n+1} \in b_j) = \sum_{i=1}^{N} P_{ij} \, \mathrm{prob}(X_n \in b_i). \tag{2}$$

Figure 1 specifically shows $\mathrm{prob}(X_{24} \in b_i)$, where $\mathrm{prob}(X_0 \in b_i) = 1/|I|$ for $b_{i \in I}$ spanning $\mathscr{I} \subset \mathscr{D}$ and 0 otherwise. Assuming $T = 5$ d, as we do here, this represents the end of nearly four months of evolution. Our transition time step choice $T = 5$ d is long enough for Markovian dynamics to approximately hold, as it is longer than the typical Lagrangian integral time scale, which is about 1 day at the ocean surface, e.g. LaCasce (2008), and as noted in pioneering (Maximenko *et al.*, 2012) and most recent work [Miron *et al.* (2017), Olascoaga *et al.* (2018), McAdam and van Sebille (2018), Miron *et al.* (2019b; 2019a; 2021), and Drouin *et al.* (2022)], involving observed, rather than simulated, trajectory data.

A critical difference between the top and middle panels of Fig. 1 is that the former uses trajectories of drifters drogued at 15 m, while the latter uses trajectories of undrogued drifters (Lumpkin *et al.*, 2012). Note that the assessment based on undrogued drifter motion (middle panel) much better resembles the GASB (bottom panel) than the assessment based on drogued drifter motion (top panel). Similar behavior has been recently reported by van Sebille *et al.* (2021) from direct inspection of individual trajectories produced by a reduced set of custom-made undrogued drifters along with drogued drifters of the GDP type. As opposed to drogued GDP drifter motion, which mostly reflects water motion at 15 m depth in the water column, undrogued drifter motion is affected by ocean current shear between 0 and 15 m, and wind and wave drag effects, mediated by "inertial" effects, i.e., those due to the buoyancy, size, and shape of the drifters (Furnans *et al.*, 2008; Beron-Vera *et al.*, 2016; 2019; Olascoaga *et al.*, 2020; Miron *et al.*, 2020b; 2020a; and Beron-Vera, 2021). The resemblance—impressively quite close—between the observed GASB distribution (in the bottom panel of Fig. 1) and that suggested by undrogued drifter trajectories indicates a dominant role of inertial effects in the drift of *Sargassum*. Indeed, these appear as an important mechanism for pelagic *Sargassum* to inundate the IAS.

The rest of this note is devoted to go beyond the discussion of direct probability density evolution with the twofold goal in mind to gain insight into: *Sargassum* connectivity as inferred by a Markov chain constructed using undrogued drifter trajectories exclusively, which show the best agreement with actual *Sargassum* movement (Sec. II); and how *Sargassum* pathways connecting a potential remote source with the IAS are accomplished in the most effective manner (Sec. III). This is done by applying specialized probabilistic tools, which are briefly reviewed before the results are discussed in each case. Section IV comments on aspects of the movement of *Sargassum* rafts that are needed to be accounted for in order to make the most out of the learnings from the analysis presented here. This brief communication is closed with a summary (Sec. V).

II. DYNAMICAL GEOGRAPHY OF SARGASSUM

Time-asymptotic aspects of the evolution along the Markov chain resulting from the discretization of the drifter motion are

encoded in the spectral properties of the transition matrix P. If every state of the chain (box of the covering) is visited irrespective of the starting state [property called *irreducibility* or *ergodicity*, and formally represented as $\forall\, i,j : b_i, b_j \in \mathscr{D}, \exists n_{ij} \in \mathbb{Z}_0^+ \backslash \{\infty\} : (P^{n_{ij}})_{ij} > 0$] and no state is revisited cyclically [property referred to as *aperiodicity* or *mixing* and expressed as $\exists i : b_i \in \mathscr{D} : \gcd\{n \in \mathbb{Z}_0^+ : (P^n)_{ii} > 0\} = 1$], then the eigenvalue $\lambda = 1$ of P is the largest possible and has multiplicity one.

The left eigenvector, $\boldsymbol{\pi}$, corresponding to $\lambda = 1$, is strictly (componentwise) positive and represents an invariant distribution (i.e., $\boldsymbol{\pi} = \boldsymbol{\pi}\mathsf{P}$), which typically reveals local maxima (bumps) where trajectories settle on in the long run. Normalizing $\boldsymbol{\pi}$ to a probability vector (i.e., such that $\sum_{i:b_i \in \mathscr{D}} \pi_i = 1$), it follows that $\boldsymbol{\pi} = \mathbf{p}\mathsf{P}^\infty$ for any probability vector $\mathbf{p}$. In other words, $\boldsymbol{\pi}$ is a limiting or *stationary distribution* that time-asymptotically sets $\mathrm{prob}(X_n \in b_i) = \pi_i$.

The right eigenvector corresponding to $\lambda = 1$ is a (column) vector of ones, denoted $\mathbf{1}$. Indeed $\mathsf{P}\mathbf{1} = \mathbf{1}$ due to (row) stochasticity of P, viz., $\sum_{j:b_j \in \mathscr{D}} P_{ij} = 1$ for all i, trivially indicating a *backward-time basin of attraction* for the time-asymptotic attractors where $\boldsymbol{\pi}$ maximizes: any probability vector with support in $\mathscr{D}$ distributes in the long run like $\boldsymbol{\pi}$.

Remark 1. The irreducibility/ergodicity and aperiodicity/mixing conditions can only be met when the flow domain $\mathscr{D}$ is closed, which is not our case. Our transition matrix is substochastic, namely, $\sum_{j:b_j \in \mathscr{D}} P_{ij} < 1$ for some i, which must be appropriately "stochasticized," for which there are several options (Froyland et al., 2014b; 2014a; and Miron et al., 2017). Here we follow Miron et al. (2021) and augment the chain by appending what has been coined by Miron et al. (2021) a two-way-nirvana state. This is
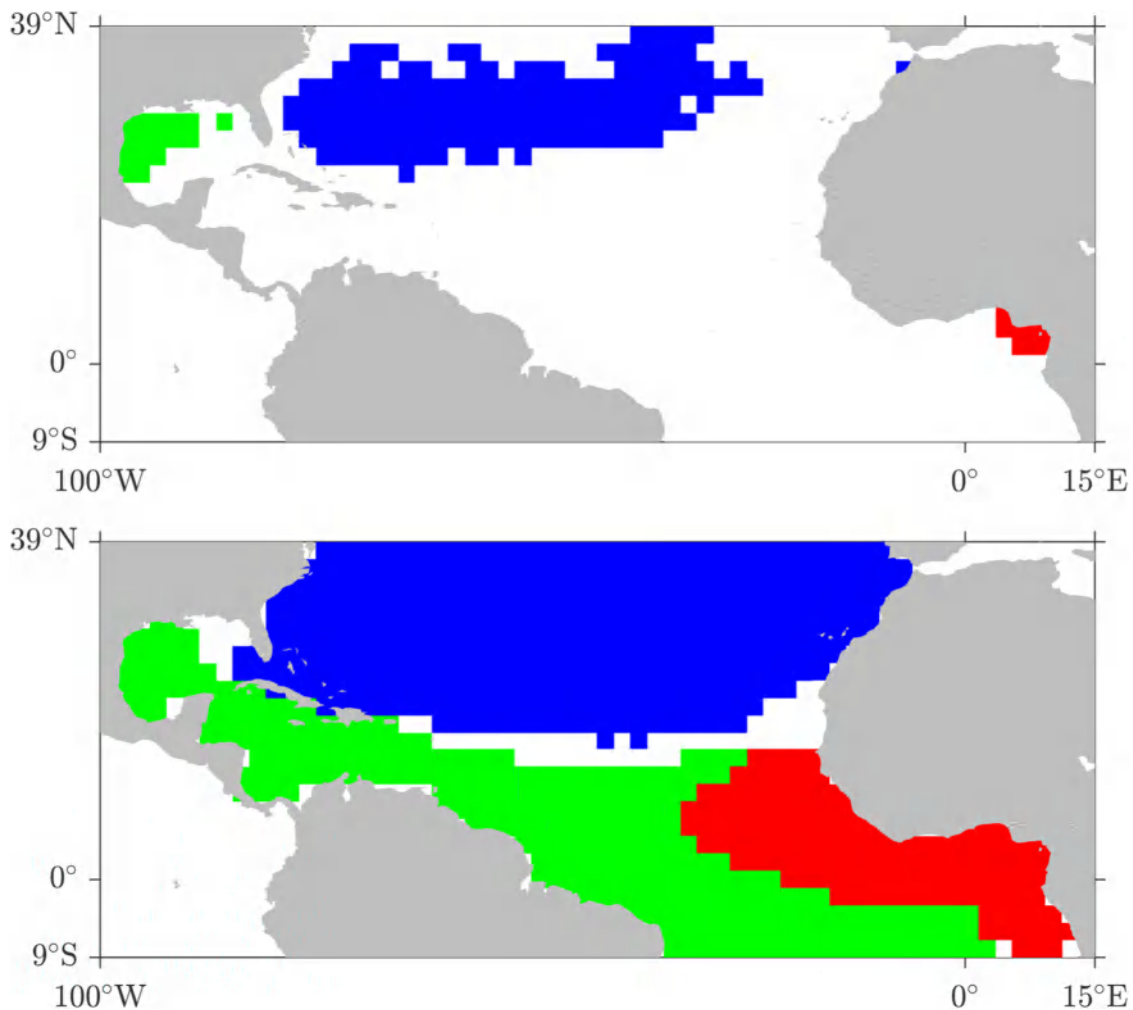
FIG. 2. (top) Almost-invariant attracting sets inferred from the spectral analysis of a transition matrix representing conditional probabilities of undrogued GDP drifters from the NOAA database to move between boxes of a grid laid down on the Atlantic Ocean domain shown. (bottom) Basins of attraction for the attractors in the top panel, i.e., the regions where trajectories, which, ending in the long run in each of the like-colored patches in the top panel, begin.

a virtual state that is appended to the chain in such a way that it compensates for any probability mass imbalances due to the openness of $\mathscr{D}$ by reinjecting them back into the chain using available trajectory information. We express this as follows. The transition matrix P computed from trajectories flowing in and out of $\mathscr{D}$, call it $\mathsf{P}^{\mathscr{D}}$, is replaced by a stochastic transition matrix $\mathsf{P} \in \mathbb{R}^{(N+1)\times(N+1)}$ defined by

$$\mathsf{P} := \begin{pmatrix} \mathsf{P}^{\mathscr{D}} & \mathbf{p}^{\mathscr{D}\to\omega} \\ \mathbf{p}^{\mathscr{D}\leftarrow\omega} & 0 \end{pmatrix}. \tag{3}$$

Here, ω is the two-way nirvana state alluded to above, used to augment the chain defined by P. In turn, vector $\mathbf{p}^{\mathscr{D}\to\omega} := (1 - \sum_{j:b_j\in\mathscr{D}} P_{ij}) \in \mathbb{R}^{N\times 1}$ gives the outflow from $\mathscr{D}$ and the probability vector $\mathbf{p}^{\mathscr{D}\leftarrow\omega} \in \mathbb{R}^{1\times N}$ gives the inflow, which is estimated from the trajectory data.

Left eigenvectors of P with λ close to 1 are signed vectors that decay at the slowest rate. The regions where P these locally maximize thus indicate *almost-invariant attracting sets*. Plateaus in the corresponding right eigenvectors highlight basins of attraction or regions where trajectories temporarily converging in the almost-invariant attractors begin. This imposes constraints on connectivity (Dellnitz and Hohmann, 1997; Dellnitz and Junge, 1999; Froyland and Dellnitz, 2003; and Koltai, 2010). The collection of nonoverlapping basins of attraction forms a partition of the dynamics into the weakly (dis)connected "provinces" of what has been termed (Froyland *et al.*, 2014b; Miron *et al.*, 2017) a *dynamical geography*, i.e., one that does not depend on arbitrary geographic demarcations but rather on the intrinsic flow characteristics of each province.

The eigenvector method, above, has been applied to surface drifter and submerged float trajectories suggesting a characterization of preferred pollution centers in the subtropical gyres (Froyland *et al.*, 2014b; Miron *et al.*, 2019b; and 2021) and in marginal seas, both at the surface (Miron *et al.*, 2017) and at depth (Miron *et al.*, 2019a), as almost-invariant attracting sets with corresponding basins of attraction spanning areas as large as those of the corresponding geographic basins, suggesting a strong influence of the regions collecting pollutants on their transport.

A similar strong influence imposed by the northwestern Gulf of Mexico, the Sargasso Sea, and the Gulf of Guinea is revealed from the analysis of our P, constructed using undrogued GDP drifter trajectories from the NOAA dataset. The top panel of Fig. 2 shows the locations where the first and second subdominant left eigenvectors of P maximize, which identify the aforementioned geographical locations as almost-invariant attracting sets. The corresponding basins of attraction, as revealed by the first and second subdominant right eigenvectors of P, are shown in the bottom panel of Fig. 2. These are depicted with the same color as the corresponding attractors to facilitate the association. [In every case, we have made use of the sparse eigenbasis approximation (Froyland *et al.*, 2019), which enables multiple feature extraction with application to coherent set identification.] Note the large geographical regions covered by the basins, which represent the domains of influence of the corresponding attractors. For instance, trajectories passing through the Caribbean Sea on their

way into the northwestern Gulf of Mexico most likely start anywhere in the Atlantic domain shown here except in the subtropical gyre. This suggests weak communication between the Sargasso Sea and the GASB region, at least for the average undrogued GDP drifter motion.

III. TRANSITION PATHS OF SARGASSUM

To unveil specific connectivity routes, additional probabilistic tools are needed. Particularly useful are those provided by the *Transition Path Theory* (*TPT*) (E and Vanden-Eijnden, 2006; Metzner *et al.*, 2009), which has been recently adapted to open dynamical systems (Miron *et al.*, 2021).

Developed to investigate rare events in complex systems, such as chemical reactions or conformation changes of molecules, TPT provides a statistical characterization of ensembles of "reactive" trajectories, namely, trajectories along which direct transitions between a source set (or "reactant") *A* and a target set (or "product") *B* in a Markov chain take place (Fig. 3).

Applications of TPT have now gone beyond the study of molecular dynamics or chemical kinetics (Noé *et al.*, 2009; Metzner *et al.*, 2006; 2009; Meng *et al.*, 2016; Thiede *et al.*, 2019; Liu *et al.*, 2019; and Strahan *et al.*, 2021). TPT has been used to shed light on pollution pathways in the ocean (Miron *et al.*, 2021), paths of the upper (Drouin *et al.*, 2022) and lower (Miron *et al.*, 2022) limbs of the overturning circulation in the Atlantic Ocean, and even
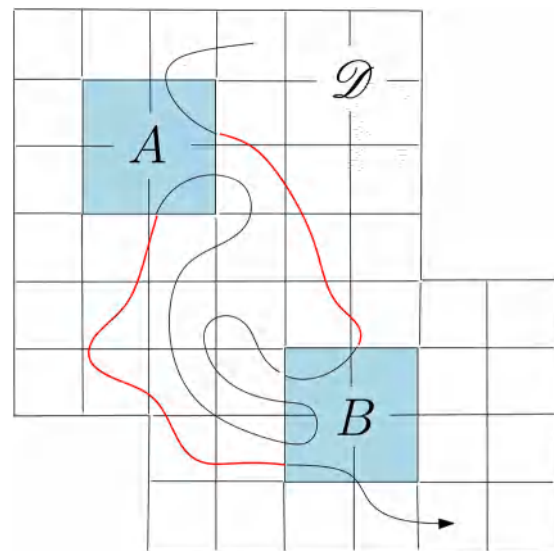
FIG. 3. Schematic representation of a piece of a hypothetical infinitely long drifter trajectory (black) that fills a closed flow domain $\mathscr{D}$, partitioned into boxes (black). Indicated are disconnected source ($A \subset \mathscr{D}$) and target ($B \subset \mathscr{D}$) sets. Highlighted in red are two members of an ensemble of reactive trajectories. These are the trajectory subpieces that connect *A* with *B* in direct transition from *A* to *B*, i.e., without returning back to *A* or going through *B* in between. The Transition Path Theory (TPT) provides a statistical characterization of the ensemble of such reactive trajectory pieces, highlighting the dominant communication conduits or transition paths between *A* to *B*.

atmospheric phenomena such as sudden stratospheric warmings (Finkel *et al.*, 2020).

The main objects of TPT are the *forward*, $\mathbf{q}^+ = (q_i^+) \in \mathbb{R}^{1 \times N}$, and *backward*, $\mathbf{q}^- = (q_i^-) \in \mathbb{R}^{1 \times N}$, *committor probabilities*. These give the probability of a random walker initially in b_i to first enter B and last exit A, respectively. The committors are fully computable from P and $\boldsymbol{\pi}$, according to

$$
\begin{cases}
\mathbf{q}^\pm\big|_{\mathscr{D} \setminus (A \cup B)} = \mathsf{P}^\pm\big|_{\mathscr{D} \setminus A \cup B, \mathscr{D}} \mathbf{q}^\pm, \\
\mathbf{q}^+\big|_A = \mathbf{0}^{|A| \times 1}, \quad \mathbf{q}^-\big|_B = \mathbf{0}^{|B| \times 1}, \\
\mathbf{q}^+\big|_B = \mathbf{1}^{|B| \times 1}, \quad \mathbf{q}^-\big|_A = \mathbf{1}^{|A| \times 1}.
\end{cases} \tag{4}
$$

Here, $\mathsf{P}^+ = \mathsf{P}$; $P_{ij}^- := \mathrm{prob}(X_n \in b_j \mid X_{n+1} \in b_i) = \frac{\pi_j}{\pi_i} P_{ji}$ are the entries of the time-reversed transition matrix, i.e., for the original chain $\{X_n\}$ traversed in backward time, $\{X_{-n}\}$; and $|_S$ denotes restriction to the subset S while $|_{S,S'}$ that to the rows corresponding to S and columns to S'.

The committor probabilities are used to express several statistics of the ensemble of reactive trajectories. The main ones are as follows:

1. The *distribution of reactive trajectories*, $\boldsymbol{\pi}^{AB} = (\pi_i^{AB}) \in \mathbb{R}^{1 \times N}$, where π_i^{AB} is defined as the joint probability that a trajectory is in box b_i while transitioning from A to B, and is computable as [Metzner *et al.* (2009) and Helfmann *et al.* (2020)]

$$
\pi_i^{AB} = q_i^- \pi_i q_i^+. \tag{5}
$$

It describes the bottlenecks during the transitions, i.e., where reactive trajectories spend most of their time. Clearly, $\pi_{i:b_i \in A \cup B}^{AB} \equiv 0$.

2. The *effective current of reactive trajectories*, $\mathsf{f}^+ = (f_{ij}^+) \in \mathbb{R}^{N \times N}$, where f_{ij}^+ gives the net flux of trajectories going through b_i at time nT and b_j at time $(n+1)T$ on their way from A to B, indicates the most likely transition channels. This is computable according to (Helfmann *et al.*, 2020)

$$
f_{ij}^+ = \max\{f_{ij}^{AB} - f_{ji}^{AB}, 0\}, \quad f_{ij}^{AB} = q_i^- \pi_i P_{ij} q_j^+. \tag{6}
$$

Remark 2. Actual paths between A and B are random, describing meanders and recirculations, but TPT concerns their average behavior, revealing the dominant transition channels from A to B. If $f_{ij}^{AB} \approx f_{ji}^{AB}$, then a lot of reactive flux is going both ways, and one can expect actual trajectories to meander and loop until getting to B. However, if $f_{ij}^{AB} \gg f_{ji}^{AB}$, then one can expect a more clear-cut flow from A to B. This is hard—if not impossible—to visualize from the direct evolution of densities (under left multiplication by P), and if the effective progression of probability mass from A to B is highly noisy, other TPT diagnostics such as the effective reactive time from A to B cannot be inferred from direct evolution.

Remark 3. An important additional observation regards TPT for open systems, as is the case of interest here with $\mathscr{D}$ representing an open flow domain. In such systems, transitions between A and B should be constrained to take place within $\mathscr{D}$, i.e., avoiding going

through ω, the (virtual) two-way nirvana state appended to compensate for probability mass imbalances (cf. Remark 1). This can be easily accomplished (Miron et al., 2021) by replacing $\boldsymbol{\pi}$ in the TPT formulas above by $\boldsymbol{\pi}|_{\mathscr{D}}$, where $\boldsymbol{\pi}$ is the stationary distribution of the transition matrix P for the closed system on $\mathscr{D} \cup \omega$, and P (in the TPT formulas) by the substochastic transition matrix $\mathsf{P}^{\mathscr{D}}$.

In the top panel of Fig. 4, we show the effective current of reactive trajectories resulting between a hypothetical source set A off West Africa (blue box) and a target set B formed by the union of boxes covering the Gulf of Mexico (red boxes) when TPT is applied on the Markov chain constructed using undrogued drifter trajectories. To visualize f^+, we follow Helfmann *et al.* (2020) and Miron *et al.* (2021) and for each b_i we estimate the vector of the average direction and the amount of the effective reactive current to each b_j, $j \neq i$. The location of A has been intentionally chosen to lie in a region near the triple boundary of the dynamical provinces (cf. Fig. 2, bottom panel), which minimizes the influence of the almost-invariant forward attractors within each basin of attraction: a probability density initialized there, in principle, has equal chance to converge, temporarily, into any of each of the three almost-attracting sets. On the other hand, placing A off West Africa as chosen finds rationale in the fact that upwelling-favorable winds there may provide the required nutrients to trigger blooming by vertical pumping them into the mixed layer. Note that the eastern extent of the GASB coincides roughly with this location (cf. Fig. 1). The bottom panel of Fig. 4 uncovers the spatial locations of the bottleneck of the transition paths, namely, where the paths spend most of their time in their direct transition from the source into the target.

Note the two routes revealed in the top panel of Fig. 4: a direct route roughly along the GASB and another more southern route, reported for the first time here, going through the Gulf of Guinea, and then passing by the mouth of the Amazon River. The southern path is strongly influenced by the almost-invariant attracting set in the Gulf of Guinea, which makes the trajectories bottleneck there. The latter is highlighted by the large values taken by the distribution of reactive trajectories in the bottom panel of Fig. 4.

Two additional TPT diagnostics are as follows:

3. The *rate of reactive trajectories* entering B (or, equivalently, exiting A), defined as the probability per time step of reactive trajectory to enter B (or exit A), which is computed as (Metzner *et al.*, 2009 and Helfmann *et al.*, 2020)

$$
k^{AB} = \sum_{i,j:b_i,b_j \in B} f_{ij}^{AB}. \tag{7}
$$

Dividing by the transition time step T, k^{AB} has the interpretation of the frequency at which a trajectory enters B (or exists A) (Miron *et al.*, 2021).

4. The *expected duration* of a transition from A to B, which is obtained by dividing the probability of a trajectory piece being reactive by the transition rate (interpreted as a frequency) (Helfmann *et al.*, 2020),

$$
t^{AB} = \frac{\sum_{j:b_j \in \mathscr{D} \setminus A \cup B} \mu_j^{AB}}{k^{AB}}. \tag{8}
$$

The computed expected duration of the transition paths into the IAS is about 12 yr, which seems rather long. However, this should not come as big surprise, given the strong influence exerted by the Gulf of Guinea almost-attracting set. In fact, if the transitions are set to avoid the basin of attraction of Gulf of Guinea attractor, the expected duration drops down to 1.8 yr or so.

Remark 4. The above requires a modification to the TPT formulas, which is achieved as follows (Miron et al., 2021). If S, S ∩ (A ∪ B) = ∅, is the set that wants to be avoided by the reactive currents, then the forward committor, $\mathbf{q}^+$ in (4), must be computed with A replaced by A ∪ S, while the backward committor, $\mathbf{q}^-$ in (4), with B replaced by B ∪ S. With these replacements, the forward committor now gives the

probability to next transition to B rather than to A or S when starting in box b_i. In turn, the backward committor gives the probability to have last come from A, not B or S. This way, the product of forward and backward committors becomes the probability when initially in b_i to have last come from A and next go to B while not passing through A, B, or S in between.

The reactive currents in the case that the basin of attraction of the Gulf of Guinea attractor is avoided reveal a single route into the IAS, roughly aligned along the GASB. The physical significance of this almost-invariant attractor is demonstrated in the top panel Fig. 5, which provides proof, independent of the Markov chain model, of the existence of such an attractor. The figure shows individual trajectories of 64 undrogued GDP drifters
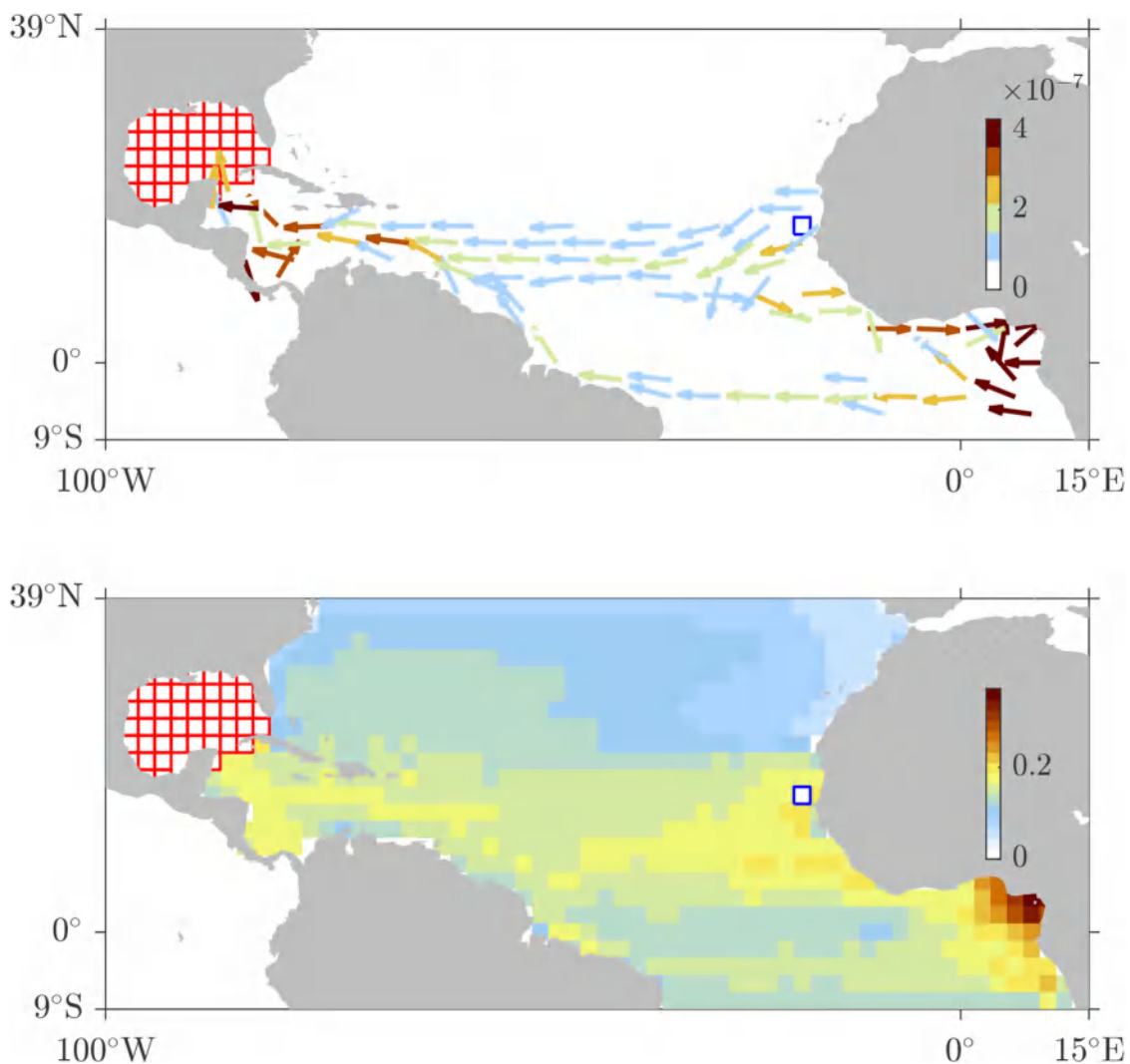

FIG. 4. (top panel) Currents of reactive trajectories between a hypothetical *Sargassum* source off West Africa and a target in the Gulf of Mexico, revealing the averaged, dominant pathways (transition paths) of *Sargassum* into the IAS. Colors represent vector magnitude. (bottom panel) Eight-root transformation of the distribution of reactive trajectories revealing where the bottlenecks of the transitions take place.
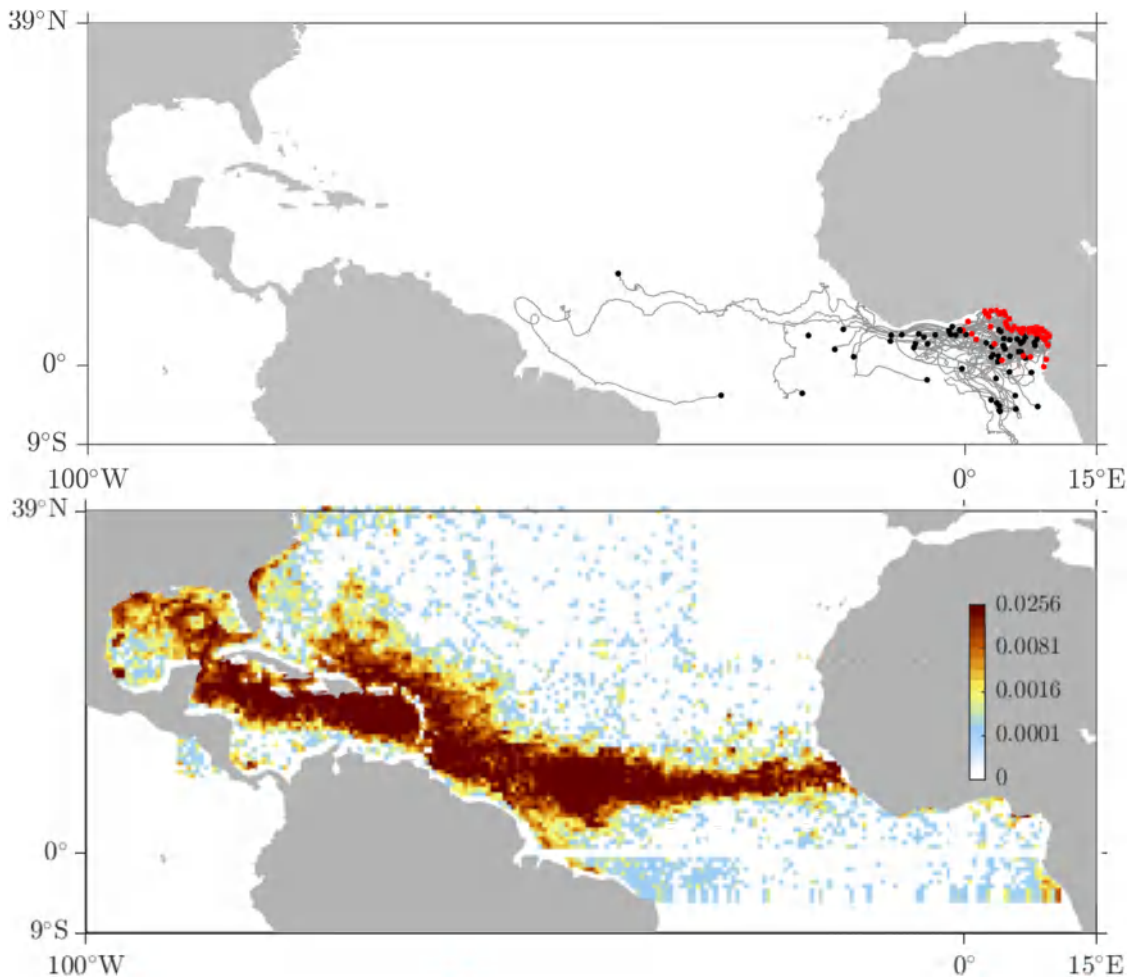
FIG. 5. (top) Trajectories of all undrogued GDP drifters from the NOAA dataset that converge in the Gulf of Guinea. Starting trajectory points are indicated by black dots, while endpoints by red dots. (bottom) Fourth-root transformation of the maximum satellite-inferred percentage of *Sargassum* coverage per pixel computed from boreal summer composites over 2011–2018.

from the NOAA database over the period 1998–2014, which were found to converge in the Gulf of Guinea. A previous TPT analysis (Miron *et al.*, 2021) had already identified the neighborhood of the Gulf of Guinea as a province for a committor-based dynamical geography for global marine debris circulation. It was also pointed out (Sutton *et al.*, 2017) that the Gulf of Guinea is a mesopelagic niche with genomic characteristics that are different than its surroundings.

The southern GASB branch unveiled by the TPT analysis does not appear to be an artifact of it. Support for the southern transition path is given in the bottom panel Fig. 5, which shows the fourth-root transformation of the quantity shown in the bottom panel of Fig. 1 computed from boreal summer composites over 2011–2018. Note the *Sargassum* presence below the equatorial line, albeit in less abundance than along the (main) GASB (branch). This is consistent with the TPT results (Fig. 4), which reveals that the southern path is weaker than the northern path, where the probability of the

reactive currents is stronger consistent with the higher concentration of satellite-inferred floating *Sargassum*.

IV. DISCUSSION

The analysis of the Markov chain model derived using undrogued drifter trajectories indicates that the combined effects of winds, waves, and surface currents can account for the basin-scale distribution of the GASB. These results are in agreement with several other studies that have suggested the importance of windage and currents in shaping the trajectories and distribution of *Sargassum* (Brooks *et al.*, 2018; Putman *et al.*, 2020; and Berline *et al.*, 2020). Our probabilistic analysis also indicates three, mostly independent, oceanographic provinces associated with aggregations of *Sargassum* that occur in the Sargasso Sea, Gulf of Guinea, and Gulf of Mexico; a finding consistent with Wang *et al.* (2019). Furthermore, our analysis suggests the

existence of a secondary pathway by which *Sargassum* is transported from the tropical Atlantic into the Caribbean Sea, south of the GASB (Figs. 4 and 5). While this pathway has not been previously described, evidence consistent with this pathway is suggested in earlier studies. Notably, Putman *et al.* (2018) showed the importance of the Guinea Current for moving *Sargassum* along the coast of northern Brazil into the Caribbean, which is fed by the South Equatorial Current. Satellite imagery depicted in Putman *et al.* (2018) and Gower *et al.* (2013) suggests that *Sargassum* enters this region from south of the equator. Thus, investigation of the ocean–atmosphere dynamics associated with this newly described southern, slower pathway for *Sargassum* and the more northern, faster GASB (Wang *et al.*, 2019), could improve the ability to predict basin-scale changes in *Sargassum* distribution, especially given very different time scales associated with the two pathways.

For instance, it may be important to consider that the North Equatorial Counter Current, running between 5 and 10°N, exhibits seasonal reversal (Lumpkin and Garzoli, 2005), which is not taken into account by our autonomous TPT analysis, wherein the transition matrix construction ignores the starting day of a drifter trajectory. To investigate the influence of the seasonal variability in our results, a nonautonomous TPT analysis will be needed. The theoretical basis for such an analysis is now available (Helfmann *et al.*, 2020), but still to be implemented. A main constraint in this case of interest is imposed by the data availability, which is unlikely to resist a seasonal partition. Simulated trajectories may serve the purpose, but this is beyond our scope here as is assessing interannual variability in *Sargassum* connectivity,

Beyond the assumed time-homogeneity, the results of this work are limited in two important counts. First is the physiological changes that *Sargassum* rafts experience as they are dragged by the combined action of ocean currents and winds, which the Markov chain model constructed here did not account for. A second aspect is the architecture of the *Sargassum* rafts, which plays a role in advection. It is well-known that finite-size or "inertial" particles, even neutrally buoyant ones, immersed in a fluid cannot adapt their velocities to the carrying flow (Maxey and Riley, 1983). Floating particle motion is further complicated by the fact that the carrying flow is not given by the ocean velocity below the sea surface itself, but by the latter plus a buoyancy-dependent fraction of the wind velocity right above the sea surface (Beron-Vera *et al.*, 2019; Olascoaga *et al.*, 2020; Miron *et al.*, 2020b; 2020a; and Beron-Vera, 2021). This aspect is implicitly accounted for by our Markov chain model as the undrogued drifters are affected by inertial effects. However, *Sargassum* rafts are not isolated inertial particles. Rather, they can be more precisely envisioned as elastic networks of buoyant inertial particles, with the buoyant inertial particles representing the gas-filled bladders connected by flexible stems that keep the rafts afloat. This was not represented by our Markov chain model. A mathematical model has been recently proposed by Beron-Vera and Miron (2020) and used Andrade-Canto *et al.*, 2022) to explain observations. This model, coupled with a physiological model of the transformations that a *Sargassum* raft experiences as it travels across regions with varying environmental conditions, would likely further elucidate the complex dynamics of *Sargassum* invasions in the IAS. Such work could further improve transport predictions by distinguishing between the roles of physical and physiological processes on observed distributions.

V. SUMMARY

In this note, we have constructed a time-homogeneous Markov chain from trajectories of undrogued drifters from the NOAA Global Drifter Program. With this tool, we found that probability density can distribute in a manner that resembled very closely the recently observed recurrent belt of high *Sargassum* concentration in the tropical Atlantic that has been termed the *Great Atlantic Sargassum Belt* (*GASB*). A spectral analysis of the associated transition matrix was further found to unveil a forward attracting almost-invariant set in the northwestern Gulf of Mexico with a corresponding basin of attraction weakly connected with the Sargasso Sea, but including the nutrient-rich regions at the outflow of the Amazon and Orinoco Rivers and also, marginally, the upwelling system off the northern coast of west Africa. This represents a data-based inference of potential remote sources of *Sargassum* recurrently invading the Intra-Americas Seas (IAS). By further applying Transition Path Theory (TPT) on the data-derived Markov chain model, two potential pathways for *Sargassum* into the IAS from the upwelling system off the coast of Africa were revealed. One TPT-inferred pathway was found to take place along the GASB. The second pathway, much slower than the GASB, was found to be more southern, first going through the Gulf of Guinea, then across the Atlantic toward the mouth of the Amazon River, and finally along the eastern South American margin. Why satellite imagery does not reveal an intense southern GASB branch needs to be investigated in view of its potentially important consequences for bloom stimulation by nutrients from river runoff. This should be done by accounting for the physiological transformations that *Sargassum* rafts are acted upon as they are transported by the combined action of currents and winds, which is the subject of ongoing research.

ACKNOWLEDGMENTS

AUTHOR DECLARATIONS

Conflict of Interest

The authors declare no competing interest.

Author Contributions

F. J. Beron-Vera: Conceptualization (equal); Formal analysis (equal); Writing – original draft (equal); Writing – review & editing (equal). **M. J. Olascoaga**: Conceptualization (supporting); Formal analysis (supporting); Writing – original draft (supporting); Writing – review & editing (supporting). **N. F. Putman**: Conceptualization (equal); Writing – review & editing (equal). **J. Triñanes**:

DATA AVAILABILITY

The data that support the findings of this study are openly available in NOAA Global Drifter Program at https://www.aoml.noaa.gov/phod/gdp/index.php (Lumpkin and Pazos, 2007) and USF and distributed by SaWS at https://optics.marine.usf.edu/projects/saws.html (Wang and Hu, 2016).

REFERENCES

Andrade-Canto, F., Beron-Vera, F. J., Goni, G. J., Karrasch, D., Olascoaga, M. J., and Triñanes, J., "Carriers of *Sargassum* and mechanism for coastal inundation in the Caribbean Sea," Phys. Fluids **34**, 016602 (2022).

Berline, L., Ody, A., Jouanno, J., Chevalier, C., André, J.-M., Thibaut, T., and Ménard, F., "Hindcasting the 2017 dispersal of *Sargassum* algae in the Tropical North Atlantic," Mar. Pollut. Bull. **158**, 111431 (2020).

Beron-Vera, F. J., "Nonlinear dynamics of inertial particles in the ocean: From drifters and floats to marine debris and *Sargassum*," Nonlinear Dyn. **103**, 1–26 (2021).

Beron-Vera, F. J. and Miron, P., "A minimal Maxey–Riley model for the drift of *Sargassum* rafts," J. Fluid Mech. **904**, A8 (2020).

Beron-Vera, F. J., Olascoaga, M. J., and Lumpkin, R., "Inertia-induced accumulation of flotsam in the subtropical gyres," Geophys. Res. Lett. **43**, 12228–12233, https://doi.org/10.1002/2016GL071443 (2016).

Beron-Vera, F. J., Olascoaga, M. J., and Miron, P., "Building a Maxey–Riley framework for surface ocean inertial particle dynamics," Phys. Fluids **31**, 096602 (2019).

Bertola, L. D., Boehm, J. T., Putman, N. F., Xue, A. T., Robinson, J. D., Harris, S., Baldwin, C. C., Overcast, I., and Hickerson, M. J., "Asymmetrical gene flow in five co-distributed syngnathids explained by ocean currents and rafting propensity," Proc. R. Soc. London, Ser. B **287**, 20200657 (2020).

Brooks, M., Coles, V., Hood, R., and Gower, J., "Factors controlling the seasonal distribution of pelagic *Sargassum*," Mar. Ecol.: Prog. Ser. **599**, 1–18 (2018).

Dellnitz, M. and Hohmann, A., "A subdivision algorithm for the computation of unstable manifolds and global attractors," Numer. Math. **75**, 293–317 (1997).

Dellnitz, M. and Junge, O., "On the approximation of complicated dynamical behavior," SIAM J. Numer. Anal. **36**, 491–515 (1999).

Drouin, K. L., Lozier, M. S., Beron-Vera, F. J., Miron, P., and Olascoaga, M. J., "Surface pathways connecting the South and North Atlantic Oceans," Geophys. Res. Lett. **49**(1), e2021GL096646, https://doi.org/10.1029/2021gl096646 (2022).

E, W. and Vanden-Eijnden, E., "Towards a theory of transition paths," J. Stat. Phys. **123**, 503–623 (2006).

Finkel, J., Abbot, D. S., and Weare, J., "Path properties of atmospheric transitions: Illustration with a low-order sudden stratospheric warming model," J. Atmos. Sci. **77**, 2327–2347 (2020).

Franks, J., Johnson, D., and Ko, D., "Pelagic *Sargassum* in the Tropical North Atlantic," Gulf Caribb. Res. **27**, C6–C11 (2016).

Froyland, G. and Dellnitz, M., "Detecting and locating near-optimal almost-invariant sets and cycles," SIAM J. Sci. Comput. **24**, 1839–1863 (2003).

Froyland, G., Pollett, P. K., and Stuart, R. M., "A closing scheme for finding almost-invariant sets in open dynamical systems," J. Comput. Dyn. **1**(1), 135 (2014a).

Froyland, G., Rock, C. P., and Sakellariou, K., "Sparse eigenbasis approximation: Multiple feature extraction across spatiotemporal scales with application to coherent set identification," Commun. Nonlinear Sci. Numer. Simul. **77**, 81–107 (2019).

Froyland, G., Stuart, R. M., and van Sebille, E., "How well-connected is the surface of the global ocean?," Chaos **24**, 033126 (2014b).

Furnans, J., Imberger, J., and Hodges, B. R., "Including drag and inertia in drifter modelling," Environ. Modell. Software **23**, 714–728 (2008).

Gower, J., Young, E., and King, S., "Satellite images suggest a new *Sargassum* source region in 2011," Remote Sens. Lett. **4**, 764–773 (2013).

Helfmann, L., Borrell, E. R., Schütte, C., and Koltai, P., "Extending transition path theory: Periodically driven and finite-time dynamics," J. Nonlinear Sci. **30**, 3321–3366 (2020).

Johns, E. M., Lumpkin, R., Putman, N. F., Smith, R. H., Muller-Karger, F. E., Rueda-Roa, D. T., Hu, C., Wang, M., Brooks, M. T., Gramer, L. J., and Werner, F. E., "The establishment of a pelagic *Sargassum* population in the tropical Atlantic: Biological consequences of a basin-scale long distance dispersal event," Prog. Oceanogr. **182**, 102269 (2020).

Jouanno, J., Benshila, R., Berline, L., Soulié, A., Radenac, M.-H., Morvan, G., Diaz, F., Sheinbaum, J., Chevalier, C., Thibaut, T., Changeux, T., Menard, F., Berthet, S., Aumont, O., Ethé, C., Nabat, P., and Mallet, M., "A NEMO-based model of *Sargassum* distribution in the tropical Atlantic: Description of the model and sensitivity analysis (NEMO-Sarg1.0)," Geosci. Model Dev. **14**(6), 4069–4086 (2021a).

Jouanno, J., Moquet, J.-S., Berline, L., Radenac, M.-H., Santini, W., Changeux, T., Thibaut, T., Podlejski, W., Ménard, F., Martinez, J.-M., Aumont, O., Shein-baum, J., Filizola, N., and N'Kaya, G. D. M., "Evolution of the riverine nutrient export to the Tropical Atlantic over the last 15 years: Is there a link with *Sargassum* proliferation?," Environ. Res. Lett. **16**, 034042 (2021b).

Koltai, P., "Efficient approximation methods for the global long-term behavior of dynamical systems – Theory, algorithms and examples," Ph.D. thesis, Technical University of Munich, 2010.

LaCasce, J. H., "Statistics from Lagrangian observations," Progr. Oceanogr. **77**, 1–29 (2008).

Lapointe, B. E., Brewton, R. A., Herren, L. W., Wang, M., McGillicuddy, D. J., Jr., Hu, C. H., Lindell, S., Hernandez, F. J., and Morton, P. L., "Nutrient content and stoichiometry of pelagic *Sargassum* reflects increasing nitrogen availability in the Atlantic Basin," Nat. Commun. **12**, 3060 (2021).

Lasota, A. and Mackey, M. C., *Chaos, Fractals and Noise: Stochastic Aspects of Dynamics*, Applied Mathematical Sciences Vol. 97, 2nd ed. (Springer, New York, 1994).

Liu, Y., Hickey, D. P., Minteer, S. D., Dickson, A., and Calabrese Barton, S., "Markov-state transition path analysis of electrostatic channeling," J. Phys. Chem. C **123**, 15284–15292 (2019).

Lumpkin, R. and Garzoli, S. L., "Near-surface circulation in the Tropical Atlantic Ocean," Deep Sea Res., Part I **52**, 495–518 (2005).

R. Lumpkin, S. A. Grodsky, L. Centurioni, M.-H. Rio, J. A. Carton, and D. Lee, "Removing spurious low-frequency variability in drifter velocities," J. Atmos. Ocean Technol. **30**, 353–360 (2012).

Lumpkin, R. and Pazos, M., "Measuring surface currents with surface velocity program drifters: The instrument, its data and some recent results," in *Lagrangian Analysis and Prediction of Coastal and Ocean Dynamics*, edited by A. Griffa, A. D. Kirwan, A. Mariano, T. Özgökmen, and T. Rossby (Cambridge University Press, 2007), Chap. II, pp. 39–67.

Maxey, M. R. and Riley, J. J., "Equation of motion for a small rigid sphere in a nonuniform flow," Phys. Fluids **26**, 883 (1983).

Maximenko, N., Hafner, J., and Niiler, P., "Pathways of marine debris derived from trajectories of Lagrangian drifters," Mar. Pollut. Bull. **65**, 51–62 (2012).

McAdam, R. and van Sebille, E., "Surface connectivity and interocean exchanges from drifter-based transition matrices," J. Geophys. Res. **123**, 514–532, https://doi.org/10.1002/2017jc013363 (2018).

Meng, Y., Shukla, D., Pande, V. S., and Roux, B., "Transition path theory analysis of c-Src kinase activation," Proc. Natl. Acad. Sci. U. S. A. **113**, 9193–9198 (2016).

Metzner, P., Schütte, C., and Vanden-Eijnden, E., "Illustration of transition path theory on a collection of simple examples," J. Chem. Phys. **125**, 084110 (2006).

Metzner, P., Schütte, C., and Vanden-Eijnden, E., "Transition path theory for Markov jump processes," SIAM J. Multiscale Model. Simul. **7**, 1192–1219 (2009).

Miron, P., Beron-Vera, F. J., Helfmann, L., and Koltai, P., "Transition paths of marine debris and the stability of the garbage patches," Chaos **31**, 033101 (2021).

Miron, P., Beron-Vera, F. J., and Olascoaga, M. J., "Transition paths of North Atlantic Deep Water," J. Atmos. Ocean Technol. **39**, 959–971 (2022).

Miron, P., Beron-Vera, F. J., Olascoaga, M. J., Froyland, G., Pérez-Brunius, P., and Sheinbaum, J., "Lagrangian geography of the deep Gulf of Mexico," J. Phys. Oceanogr. **49**, 269–290 (2019a).

Miron, P., Beron-Vera, F. J., Olascoaga, M. J., and Koltai, P., "Markov-chain-inspired search for MH370," Chaos **29**, 041105 (2019b).

Miron, P., Beron-Vera, F. J., Olascoaga, M. J., Sheinbaum, J., Pérez-Brunius, P., and Froyland, G., "Lagrangian dynamical geography of the Gulf of Mexico," Sci. Rep. **7**, 7021 (2017).

Miron, P., Medina, S., Olascoaga, M. J., and Beron-Vera, F. J., "Laboratory verification of a Maxey–Riley theory for inertial ocean dynamics," Phys. Fluids **32**, 071703 (2020a).

Miron, P., Olascoaga, M. J., Beron-Vera, F. J., Triñanes, J., Putman, N. F., Lumpkin, R., and Goni, G. J., "Clustering of marine-debris-and *Sargassum*-like drifters explained by inertial particle dynamics," Geophys. Res. Lett. **47**, e2020GL089874, https://doi.org/10.1029/2020gl089874 (2020b).

Noé, F., Schütte, C., Vanden-Eijnden, E., Reich, L., and Weikl, T. R., "Constructing the equilibrium ensemble of folding pathways from short off-equilibrium simulations," Proc. Natl. Acad. Sci. U. S. A. **106**, 19011–19016 (2009).

Norris, J., *Markov Chains* (Cambridge University Press, 1998).

Olascoaga, M. J., Beron-Vera, F. J., Miron, P., Triñanes, J., Putman, N. F., Lumpkin, R., and Goni, G. J., "Observation and quantification of inertial effects on the drift of floating objects at the ocean surface," Phys. Fluids **32**, 026601 (2020).

Olascoaga, M. J., Miron, P., Paris, C., Pérez-Brunius, P., Pérez-Portela, R., Smith, R. H., and Vaz, A., "Connectivity of Pulley Ridge with remote locations as inferred from satellite-tracked drifter trajectories," J. Geophys. Res. **123**, 5742–5750, https://doi.org/10.1029/2018jc014057 (2018).

Paraguay-Delgado, F., Carreño-Gallardo, C., Estrada-Guel, I., Zabala-Arceo, A., Martinez-Rodriguez, H. A., and Lardizábal-Gutierrez, D., "Pelagic *Sargassum* spp. capture CO_2 and produce calcite," Environ. Sci. Pollut. Res. **27**, 25794 (2020).

Putman, N. F., Goni, G. J., Gramer, L. J., Hu, C., Johns, E. M., Trinanes, J., and Wang, M., "Simulating transport pathways of pelagic *Sargassum* from the Equatorial Atlantic into the Caribbean Sea," Prog. Oceanogr. **165**, 205–214 (2018).

Putman, N. F., Lumpkin, R., Olascoaga, M. J., Trinanes, J., and Goni, G. J., "Improving transport predictions of pelagic *Sargassum*," J. Exp. Mar. Biol. Ecol. **529**, 151398 (2020).

Resiere, D., Valentino, R., Nevière, R., Banydeen, R., Gueye, P., Florentin, J., Cabié, A., Lebrun, T., Mégarbane, B., Guerrier, G., and Mehdaoui, H., "*Sargassum* seaweed on Caribbean islands: An international public health concern," Lancet **392**, 2691 (2018).

Smetacek, V. and Zingone, A., "Green and golden seaweed tides on the rise," Nature **504**, 84–88 (2013).

Strahan, J., Antoszewski, A., Lorpaiboon, C., Vani, B. P., Weare, J., and Dinner, A. R., "Long-time-scale predictions from short-trajectory data: A benchmark analysis of the trp-cage miniprotein," J. Chem. Theory Comput. **17**, 2948–2963 (2021).

Sutton, T. T., Clark, M. R., Dunn, D. C., Halpin, P. N., Rogers, A. D., Guinotte, J., Bograd, S. J., Angel, M. V., Perez, J. A. A., Wishner, K., Haedrich, R. L., Lindsay, D. J., Drazen, J. C., Vereshchaka, A., Piatkowski, U., Morato, T., Błachowiak-Samołyk, K., Robison, B. H., Gjerde, K. M., Pierrot-Bults, A., Bernal, P., Reygondeau, G., and Heino, M., "A global biogeographic classification of the mesopelagic zone," Deep Sea Res., Part I **126**, 85–102 (2017).

Thiede, E. H., Giannakis, D., Dinner, A. R., and Weare, J., "Galerkin approximation of dynamical quantities using trajectory data," J. Chem. Phys. **150**, 244111 (2019).

Ulam, S. M., *A Collection of Mathematical Problems* (Interscience, 1960).

van Sebille, E., Zettler, E., Wienders, N., Amaral-Zettler, L., Elipot, S., and Lumpkin, R., "Dispersion of surface drifters in the tropical Atlantic," Front. Mar. Sci. **7**, 607426 (2021).

van Tussenbroek, B. I., Hernández Arana, H. A., Rodríguez-Martínez, R. E., Espinoza-Avalos, J., Canizales-Flores, H. M., González-Godoy, C. E., Barba-Santos, M. G., Vega-Zepeda, A., and Collado-Vides, L., "Severe impacts of brown tides caused by *Sargassum* spp. on near-shore Caribbean seagrass communities," Mar. Pollut. Bull. **122**, 272–281 (2017).

Wang, M. and Hu, C., "Mapping and quantifying *Sargassum* distribution and coverage in the Central West Atlantic using MODIS observations," Remote Sens. Environ. **183**, 350–367 (2016).

Wang, M., Hu, C., Barnes, B. B., Mitchum, G., Lapointe, B., and Montoya, J. P., "The great Atlantic *Sargassum* belt," Science **365**, 83–87 (2019).